RSC Advances

ROYAL SOCIETY OF CHEMISTRY

www.rsc.org/advances

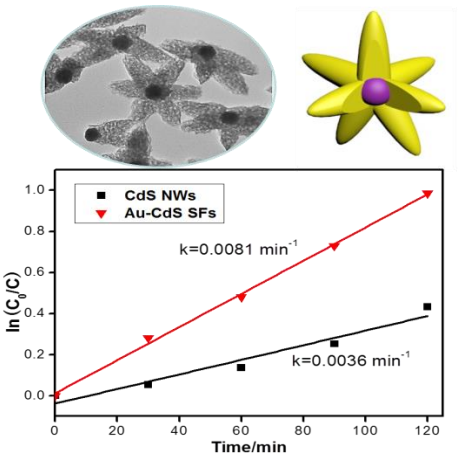

A novel starfish-like Au-CdS heterostructures are constructed by a simple self-assembling method with centered Au nanoparticles, and exhibit highly efficient visible light photodegradation of organic dyes.

Journal Name

RSCPublishing

COMMUNICATION

Cite this: DOI: 10.1039/x0xx00000x

Starfish-like Au-CdS hybrids for high efficient photocatalytic degradation of organic dyes

Received ooth January 2012,
Accepted ooth January 2012

DOI: 10.1039/x0xx00000x

www.rsc.org/

Xinyu Wang, Yingyu Long, Leijia Huan, Pan Hu and Xinsheng Peng*[a,b]

Starfish-like Au-CdS hybrids were prepared through a simple self-assembling method at room temperature, which demonstrated high efficient photocatalytic degradation of organic dyes, due to the enhancement of visible light absorption and charge separation.

Over the past several decades, semiconductor photocatalysts have attracted wide-range attention for the degradation of organic dyes and hydrogen evolution.[1-4] As a promising visible-light semiconductor photocatalyst, CdS (E_g = 2.4 eV) has an apparent advantage over TiO_2,[5] which can only work under UV light. With the excellent absorption of visible light, there have been many reports on morphology-dependent properties of CdS.[6-7] Unfortunately, being a single component, the photocatalytic efficiency of CdS is low, owing to the fast recombination of photoinduced electrons and holes.[8-9] Many efforts have been done to improve the photocatalytic efficiency of CdS, by constructing hetero hybrids, such as Au-CdS hybrids,[8] graphene-CdS hybrids,[10] and ZnS-CdS hybrids.[11]

Different systems of metal-semiconductor (M-S) hybrids have been reported, such as Pt-TiO_2,[12] Au-TiO_2,[13] Au-Bi_2S_3,[14] Au-CdS,[9] Au-CdSe[15]. These hybrids present more outstanding photocatalytic performances than the single metal or semiconductor, for the efficient charge transfer between metal and semiconductor. However, the synthesis of the hybrids is not easy. Generally, metal can be deposited on the surface of semiconductor by many methods, e.g., photodeposition,[16] microwave-assisted chemical reduction[17] and electrostatic attraction.[18] But irregular structure and aggregation of metal or semiconductor often observed which restrict the photocatalytic efficiency of the hybrids. Nevertheless, there were many previous reports about M-S hybrids with abrupt heterostructure and excellent properties on photoelectricity and photocatalysis.[19-21] Most of these M-S structures were zero-dimensional or one-dimensional, nanodumbbells,[19] semiconductor rods with metal tips,[20] or just nanoparticles.[9] There were few reports about three-dimensional M-S structures, such as pentapod Au-CdSe nanostructure[15] and tetrapod Au-CdS.[22]

In this work, starfish-like Au-CdS hybrids (SFs) are prepared by a simple self-assembly method at room temperature. Briefly, Au-$Cd(OH)_2$ SFs are obtained by assembling negatively charged Au nanoparticles (NPs) with positively charged $Cd(OH)_2$ nanowires (NWs), and then converted into Au-CdS SFs by H_2S. To the best of our knowledge, this is the first report about Au-CdS SFs. To explore the optical properties of the prepared Au-CdS SFs, UV absorption, photoluminescence (PL) and the photodegradation of RhB were carried out. The Au-CdS SFs exhibit high photocatalytic efficiency for RhB. This report provides an easy way to prepare M-S hybrids for the application in many fields, e.g., photodetectors, optoelectronics and hydrogen production.[23-25]

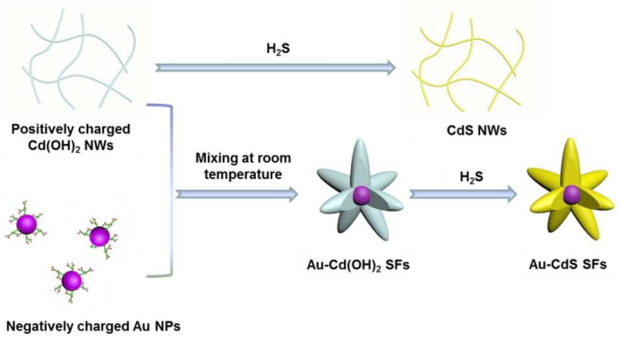

Fig. 1 Schematic illustration of the synthesis of CdS NWs and Au-CdS SFs by a simple self-assembly method.

For comparison, CdS NWs were obtained as a result of the vulcanization of $Cd(OH)_2$ NWs in H_2S gas. Au-$Cd(OH)_2$ SFs were synthesized by assembling positively charged $Cd(OH)_2$ NWs and negatively charged 40 nm Au NPs. After that Au-$Cd(OH)_2$ SFs were converted into Au-CdS SFs. A typical SEM image of $Cd(OH)_2$ NWs is shown in Fig. 2a. These nanostructures have an average diameter of about 1.9 nm and length of about few micrometers.[26] Moreover, these cadmium hydroxide NWs are highly positively charged.[26]

Negatively charged Au NPs with a mean size of 40 nm were obtained from BBI solution without further treatment. As described in the Fig. 1, the Au NPs and $Cd(OH)_2$ NWs were blended together. Fig. 2b shows the typical structure of Au-$Cd(OH)_2$ hybrids. The detailed structure of the SFs hybrids can be observed in the inset of Fig. 2b, in which Au NPs occupy the center and the arms are composed by $Cd(OH)_2$ NWs.

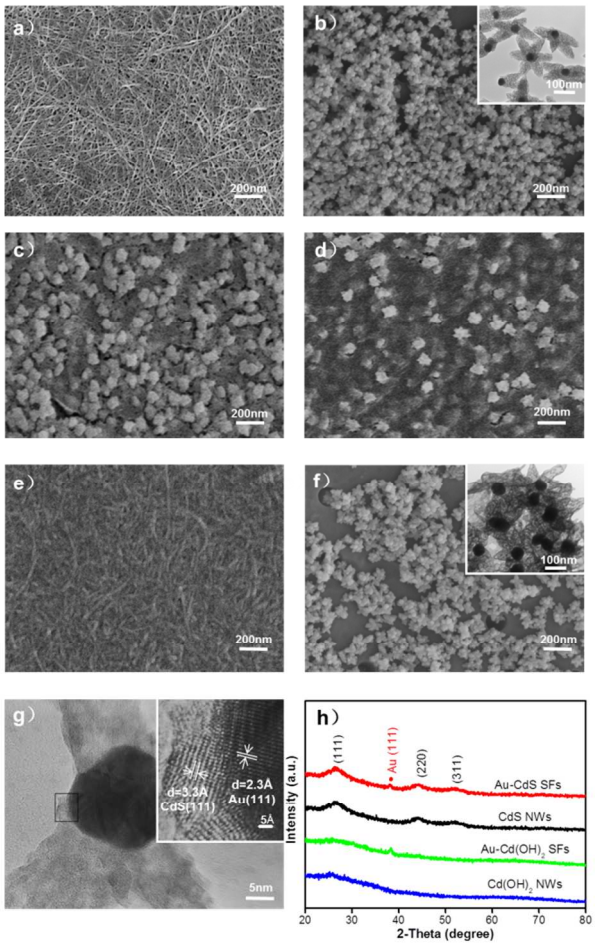

Fig. 2 SEM images of (a) $Cd(OH)_2$ NWs, and (b-d) Au-$Cd(OH)_2$ hybrids with the ratios of 2:1, 5:1 and 10:1, respectively. (e) SEM image of CdS NWs. (f) SEM image of Au-CdS SFs. Inset: TEM image of Au-CdS SFs. (g) HRTEM of Au-CdS SFs，the inset corresponds to the lattice fringes of the black frame. And (h) XRD patterns of $Cd(OH)_2$ NWs, Au-$Cd(OH)_2$ SFs, CdS NWs and Au-CdS SFs.

To study the optimal formation parameters of the SFs, different volume ratios of Au NPs colloids to $Cd(OH)_2$ NWs solution were employed, as shown in Fig. 2(b-d). Normally, with increase volume of $Cd(OH)_2$ NWs, the SFs become bigger, while more and more $Cd(OH)_2$ NWs are remained. It demonstrates the fact that every Au NPs can only attract a certain number of $Cd(OH)_2$ NWs, due to the limited surface area and charges. When different volume ratios of Au NPs colloids and $Cd(OH)_2$ NWs solution are used, Au-$Cd(OH)_2$ SFs are obtained at the ratio of 1:2 (Fig. 2b); Au-$Cd(OH)_2$ SFs and $Cd(OH)_2$ NWs are observed at the ratios of both 1:5 and 1:10 (Fig. 2(c-d)), showing that there are excess $Cd(OH)_2$ NWs; Au-$Cd(OH)_2$ SFs are not obtained at the volume ratio of 2:1 (Fig. S2) for the lack of $Cd(OH)_2$ NWs.

In our system, we found that in the case of Au NPs with size of 5 nm, 20 nm, 80 nm and 100 nm, no SFs were obtained. This means only when the size of Au NPs reaches a certain value, the SFs come into being. The negatively charged Au NPs draw the positively $Cd(OH)_2$ NWs by electrostatic attraction. With a relative large surface area of Au NPs, tens of $Cd(OH)_2$ NWs can gather to form a big architecture as the arms of SFs. At the same time, with the stirring of the solution and the electrostatic force with Au NPs and $Cd(OH)_2$ NWs, the nanowires disintegrate into small parts with length of about 100 nm. Then Au-$Cd(OH)_2$ SFs are formed. The as-synthetized Au-$Cd(OH)_2$ SFs are then filtered on a porous PC membrane. To obtain Au-CdS SFs, the PC membrane is put into an atmosphere with H_2S.[27]

Fig. 2h shows the XRD patterns of Au-CdS SFs and CdS NWs, respectively. The diffraction peaks of the as-synthesized CdS correspond to the cubic phase of CdS (JPCDS. 80-0019), which are (111), (220), (311). For Au-CdS, the diffraction is similar to that of CdS except the diffraction peak at 38.2º which is assigned to (111) plane (JPCDS. 04-0784). Fig. 2g shows the high resolution transmission electron microscopy (HRTEM) image of Au-CdS SFs, in which Au and CdS can be distinguished clearly. The lattice fringes of Au with a distance of 2.3 Å, is assigned to the plane of Au (111); and that of CdS with a distance of 3.3 Å is assigned to CdS (111) plane. The result is cohering with that of XRD result.

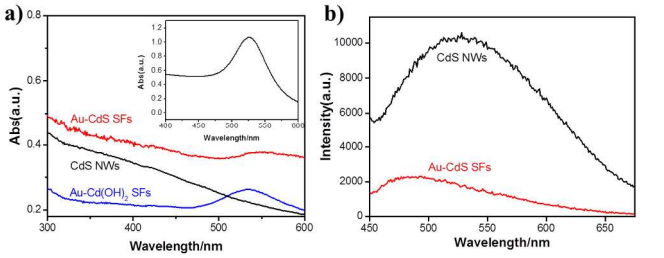

Fig. 3 (a) The UV-visible absorption spectra of CdS NWs , Au-CdS SFs and Au-$Cd(OH)_2$ SFs. Inset is the absorption of Au nanoparticles with a size of 40 nm. (b) PL spectra of CdS NWs and Au-CdS SFs.

One of the pivotal features of M-S is the optical-absorption spectra. [28] As shown in Fig. 3a, the surface plasmon resonance (SPR) absorption peak of Au-CdS SFs turns to be wider and also performs some redshift, which is a generic phenomenon of such hybrids.[14] The exciton-plasmon coupling and the high dielectric coefficient of the CdS is the reason for the result. However such phenomenon is not observed in the Au-$Cd(OH)_2$ SFs. Moreover, compared to single CdS NWs, Au-CdS SFs display an enhanced absorption of a wide range of light (300 - 600 nm), which is aroused by the field enhancement.[29] The enhanced absorption of light can promote the number of photogenerated carriers, which can further enhance the photocatalytic efficiency.[13]

The PL spectra of CdS NWs and Au-CdS SFs are shown in Fig. 3b. There is a notable quenching of CdS PL emission at the peak of 520 nm because of the efficient separation of photogenerated electrons and holes. With a lower Fermi energy level, Au NPs can capture photogenerated electrons easily, which leads to the decrease of radiative recombination. Such electron transfer from CdS to Au

can enhance the photocatalytic performance. Similar phenomena have been observed in many M-S hybrids, such as Au-CdSe[15] and Au-TiO_2[30] nanostructures. In addition, the quenching of CdS PL emission can also be induced by the surface plasmon absorption,[31] since the absorption peak of Au NPs and the emission peak of CdS are close.

To confirm the electron transfer process in Au-CdS SFs, the decay times of CdS NWs and Au-CdS SFs were measured and shown in Fig. 4a. The curves are fitted as cubic functions, and accordingly the exaction lifetime of CdS and Au-CdS are calculated. The CdS NWs has a lifetime of 76.19 ns and Au-CdS SFs has a lifetime of 53.95 ns. In the process of excitonic recombination, Au NPs provide a lower barrier for photogenerated electron to return to ground state than that of CdS NWs. The shortening of the decay time indicates the electron transfer from CdS to Au.[15]

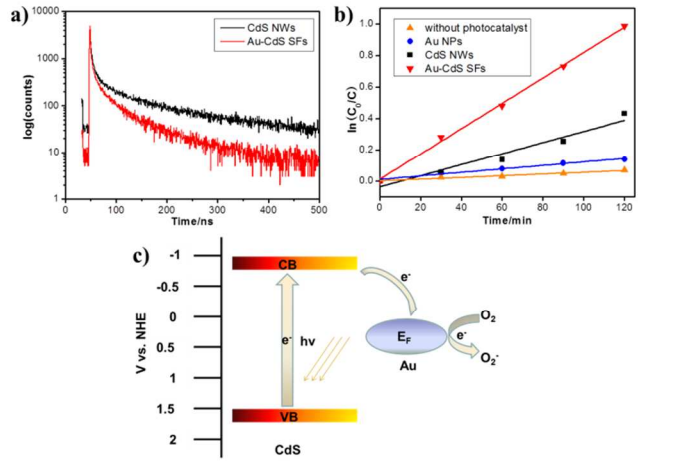

Fig. 4 (a) The decay profiles of CdS NWs and Au-CdS SFs. (b) The rate of photodegradation of RhB dye under visible-light in presence of Au NPs (k_1=0.0011 min^{-1}), CdS NWs (k_2=0.0036 min^{-1}), Au-CdS SFs (k_3=0.0081 min^{-1}) and without photocatalyst (k_0=0.0005 min^{-1}). And (c) Schematic of the band alignment and charges transfer between CdS and Au (NHE is the normal hydrogen electrode, CB is conduction band, VB is valence band).

The enhanced separation of photogenerated electron and hole pairs in Au-CdS SFs is desirable for photocatalytic oxidizing degradation of organic dye under visible-light.[9] The photocatalytic degradation of RhB by CdS NWs and Au-CdS SFs are explored under visible light, respectively. For comparison, the photocatalytic degradation of RhB by Au NPs is also performed. 30% of RhB are degraded in the presence of CdS NWs only, and just 10% of RhB are degraded by Au NPs after 2 hours. In the case of Au-CdS SFs, 65% of RhB are degraded, which is much higher than that of CdS NWs. The reaction rate constants (shown in Fig. 4b) are also calculated based on the first-order kinetic model. The degradation of RhB can be expressed by $\ln (C_0/C) = kt$, where C_0 is the initial concentration of RhB, C is the concentration of RhB at the time t, and k is the rate constant. The rate constant for CdS NWs is 0.0036 min^{-1} and that of Au-CdS SFs is 0.0081 min^{-1}, which distinctly demonstrates the higher photocatalytic efficiency of Au-CdS SFs. The photocatalytic activity of different Au/CdS hybrids prepared from different volume ratios of Au colloids and $Cd(OH)_2$ NWs solution is shown in Fig. S5. As described above, only Au-CdS SFs are formed when the volume ratio of Au colloids to $Cd(OH)_2$ NWs solution is 1:2. However, if this ratio changes to 1:5 and 1:10, respectively, excess CdS NWs are observed, except Au-CdS SFs, and resulting in lower photocatalytic efficiency. When the volume ratio of Au colloids to $Cd(OH)_2$ NWs solution is 2:1, excess Au NPs and few Au-CdS hybrids are appeared (not SFs). Again this sample presents lower photocatalytic efficiency than that of Au-CdS SFs. It is clear that the Au-CdS SFs presents the best photocatalytic performance for RhB. This efficiency was higher than that of CdS QDs–Au NPs@POM (polyoxometalate) composites,[9] and comparable to that of CdS QDs-Au composites.[8]

To better understand the photodegradation mechanism of such heterostructures, the band structures of CdS-Au SFs are shown in Fig. 4c, the conduction band of CdS is higher than the Fermi energy of Au.[14, 32] When the CdS generates electrons from valence band to conduction, electrons tend to flow toward Au NPs, enhancing the separation of photogenerated electrons and holes, which accords with the quenching of PL and shortening of decay time. The holes with strong oxidizing property in the CdS valence band and the electrons which react with oxygen to form oxidized media (O^{2-}) in the Au NPs can promote the efficiency of as-synthesized hybrids.[8] In addition, as we observe in the UV-Visible profile, the enhancement of the absorption of visible-light raise the amount of photoinduced carriers, resulting in a better performance of photocatalytic activities.

Conclusions

In summary, a simple method is developed to prepare Au-CdS SFs with Au core and CdS arms. The as-prepared Au-CdS SFs performed higher photocatalytic efficiency than that of CdS NWs, due to M-S heterostructures. Photoinduced electrons can migrate from CdS arms to the Au NPs, which enhances the separation of electron-hole pairs and the efficiency of photocatalysis. The increase of the absorption of light from 300 to 600 nm can also promote the property of photocatalysis. Our method provides a pathway to explore new hybrids for visible light photocatalysis, photovoltaic devices and so on. Other systems, such as Au-ZnS, Au-CdSe, and Au-ZnSe, are being developed in our group.

Acknowledgements

This work was supported the National Natural, Science Foundations of China (NSFC 21271154), Natural Science Foundation for Outstanding Young Scientist of Zhejiang Province (LR14E020001), and Doctoral Fund of Ministry of Education of China (20110101110028),

Notes and references

[a]*State Key Laboratory of Silicon Materials, Department of Materials Science and Engineering, Zhejiang University, China.* [b]*Cyrus Tang Center for Sensor Materials and Applications, Zhejiang University, Hangzhou 310027, China.*
E-mail: pengxinsheng@zju.edu.cn

1 Z. G. Zou, J. H. Ye, K. Sayama, H. Arakawa, *Nature*, 2001, **414**, 625.
2 N. Z. Bao, L. M. Shen, K. Domen, *Chem. Mater.*, 2008, **20**, 110.
3 M. R. Hoffmann, S. T. Martin, D. W. Bahnemann, *Chem. Rev.*, 1995, **95**, 69.

4 A. L. Linsebigler, G. Q. Lu, J. T. Yates, *Chem. Rev.*, 1995, **95**, 735.
5 P. Roy, S. Berger, P. Schmuki, *Angew. Chem. Int. Ed.*, 2011, **50**, 2904.
6 B. C. Pan, Y. M. Xie, S. J. Zhang, L. Lv, W. M. Zhang. *ACS Appl. Mater. Interfaces*, 2012, **4**, 3938.
7 D. W. Jing, L. J. Guo, *J. Phys. Chem. B*, 2006, **110**, 11139.
8 S. C. Han, L. F. Hu, N. Gao, A. A. Al-Ghamdi, X. S. Fang, *Adv. Funct. Mater.*, 2014, **10**, 1.
9 X. L. Xing, R. J. Liu, X. L. Yu, G. J. Zhang, H. B. Cao, J. N. Yao, B. Z. Ren, Z. X. Jiang, H. Zhao, *J. Mater. Chem. A*, 2013, **1**, 1488.
10 N. Zhang, Y. H. Zhang, X. Y. Pan, X. Z. Fu, S. Q. Liu, Y. J. Xu, *J. Phys. Chem. C*, 2011, **115**, 23501.
11 J. Zhang, J. G. Yu, Y. M. Zhang, Q. Li, J. R. Gong, *Nano Lett.*, 2011, **11**, 4774.
12 X. B. Chen, L. Liu, P. Y. Yu, S. S. Mao, *Science*, 2011, **331**, 746.
13 H. X. Li, Z. F. Bian, J. Zhu, Y. N. Huo, H. Li, Y. F. Lu. *J. Am. Chem. Soc.*, 2007, **129**, 4538-4539.
14 G. Manna, R. Bose, N. Pradhan, *Angew. Chem. Int. Ed.*, 2014, **53**, 1.
15 K. K. Haldar, G. Sinha, J. Lahtinen, A. Patra, *ACS Appl. Mater. Interfaces*, 2012, **4**, 6266.
16 C. Pacholski, A. Kornowski, H. Weller, *Angew. Chem. Int. Ed*. 2004, **43**, 4774.
17 E. Z. Liu, L. M. Kang, Y. H. Yang, T. Sun, X. Y. Hu, H. C. Liu, Q. P. Wang, X. H. Li, J. Fan, *Nanotechnology*, 2014, **25**, 1.
18 S. Q. Liu, Y. J. Xu, *Nanoscale*, 2013, **5**, 9330.
19 H. Y. Lin, Y. F. Chen, *Appl. Phys. Lett*, 2006, **88**, 161911.
20 D. Mongin, E. Shaviv, P. Maioli, A. Crut, U. Banin, N. D. Fatti, F. Vallee, *ACS Nano*, 2012, **6**, 7034.
21 T. Mokari, E. Rothenberg, I. Popov, R. Costi, U. Banin, *Science*, 2004, **304**, 1787.
22 A. Figuerola, M. V. Huis, M. Zanella, A. Genovese, S. Marras, A. Falqui, H. W. Zandbergen, R. Cingolani, L. Manna, *Nano Lett.*, 2010, **10**, 3028.
23 K. M. Deng, L. Li, *Adv. Mater.*, 2014, **26**, 2619.
24 H. Q. Li, X. Wang, J. Q. Xu, Q. Zhang, Y. Bando, D. Golberg, Y. Ma, T. Y. Zhai, *Adv. Mater.*, 2013, **25**, 3017.
25 H. J. Yan, J. H. Yang, G. J. Ma, G. P. Wu, X. Zong, Z. B. Lei, J. Y. Shi, C. Li, *J. Catal.,* 2009, **266**, 165.
26 I. Ichinose, K. Kurashima, T. Kunitake, *J. Am. Chem. Soc.*, 2004, **126**, 7162.
27 M. F. Zhang, M. Drechsler, A. H. E. Muller, *Chem, Mater.*, 2004, **16**, 537.
28 J. S. Lee, M. I. Bodnarchuk, E. V. Shevchenko, D.V. Talapin, *J. Am. Chem. Soc.*, 2010, **132**, 6382.
29 K. Tanabe, *J. Phys. Chem. C*, 2008, **112**, 15721.
30 J. Kim, D. Lee, *J. Am. Chem. Soc.*, 2007, **129**, 7706.
31 J. R. Lakowicz, *Anal. Biochem.*, 2005, **337**, 171.
32 F. Zhen, Y. F. Liu, Y. T .Fan, Y. H. Ni, X. W. Wei, K. B. Tang, J. M. Shen, Y. Chen, *J. Phys. Chem. C*, 2011, **115**, 13968.

